Ag_2Te thin films' structural and optical characteristics as a result of Al doping

Liqaa S. Ali*, Aliyah A. Shihab
Department of physics, College of Education for Pure Science / Ibn Al-Haitham, University of Baghdad, Baghdad, Iraq

During the course of this investigation, Ag2Te and Al-doped Ag2Te films' structural and optical properties at various concentrations (1%, 1.5%) are examined. The thermal evaporation method was used to deposit 400-nm thick Ag2Te thin films on glass substrates at 100 °C. The structure is monoclinic of the polycrystalline films were revealed by (XRD). Between 1 and 1.5%, the activated precursor did not vary with respect to the favored direction. According to the XRD results, the mean crystal sizes ranged from 25.62 to 37.13 nm. The surface of the film is incredibly smooth, according to atomic force microscope study (AFM). The produced films' optical characteristics were investigated. optical absorption coefficient (α) of films were determined using the absorption spectra within the wavelength region (400-1000) nm. It was discovered that the optical energy gap allows direct transmission and that it narrows with doping.. AFM was used to measure the grain size and roughness, which change when impurities are added.

(Received May 15, 2023; Accepted August 7, 2023)

Keywords: Ag_2Te thin films, Al, Thermal evaporation, Doping elements, AFM

1. Introduction

Superionic conductivity and structural transitions in phase are two unique features of the I-VI semiconductor compound known as silver telluride[1]. The monoclinic structure of silver telluride at a low temperature changes structurally to the cubic structure at a high temperature[2]. It has a molar mass of 341.3364 g/mol and a density of 8.318 g/cm^3, a large magnetoresistance, and high electrical conductivity. It is a mixed ionic conductor with a high concentration[3]. The Quantum size effects have caused binary chalcogenide semiconductors to exhibit size-dependent optical characteristics[4]. It has numerous applications in nonlinear optical devices and switching devices. electrochemical potential memory devices [5] .Schottky barrier[6]. the photodetector, solar energy conversion, switching devices, superionic conductors [7]. Magnetic field sensing devices, and semiconducting optical device for the visible region. The crystalline structure has a monoclinic[8]. Ag_2Te numerous techniques to prepare it, the like hydrothermal, co-precipitation, sol_gel, and sonochemical, and deposited through heating, chemical bath deposition, solid vapor phase interaction, and vacuum evaporation the mixture of the Ag and Te at high temperature [9, 10].

2. Experimental

Ag and Te were combined to create alloys with a purity of 99.999%. Ag and Te each have a weight percentage of 1.885 gm and 1.114 gm, respectively. Then they thoroughly combined with one another in pristine quartz tubes. The tubes were sealed at a pressure of 10^{-3} Torr. The tubes were put into containers and then put in an electric furnace. Stepwise temperature increases of 5 °C/min were made up to a final temperature of 1000 °C when the samples were kept for 5 hours[11]. The ingots were removed from the tubes and thoroughly ground before being used to produce thin films on glass substrates for cleaning at room temperature. Using the thermal

* Corresponding author: liqaa.sadiq1004@ihcoedu.uobaghdad.edu.iq
https://doi.org/10.15251/JOR.2023.194.433

evaporation process in a 10^{-5} Torr vacuum. The thickness of them is (400±20).with rate of deposition (2.07813nm Sec^{-1})[12]. By using the thermal evaporation method, the Ag_2Te films were doped with the element (Al) in a ratio of (1%, 1.5%). After determining the atomic percentages, the doping element was deposited on the Ag_2Te films, and the samples were then placed in an electric furnace at 100 °C for one hour[13].

3. Results and discussion

3.1. Structural properties

Figure 1**:** depicts XRD spectra of the films that were applied at a thickness of 400 nm and a temperature of 100 °C on a clean glass substrate. It was found that the pure films of (Ag_2Te) and Al-doped polycrystalline. as is typical, and had seven diffraction peaks. and the monoclinic phase's (200),(-112), (211), (-133), (-321),(020) and (013) planes (JCPOS 01-081-1985). The XRD results demonstrated that, in comparison to pure Ag_2Te, the peak intensity increases as aluminum doping concentration increases[14]. This demonstrates that an decrease in FWHM may result in an increase in the crystallization rate.

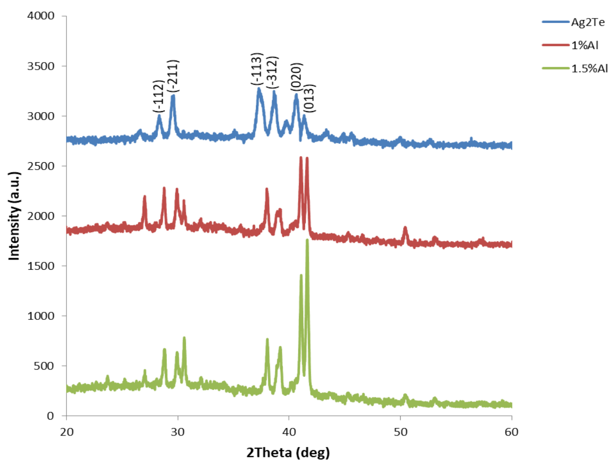

Fig. 1. All prepared film XRD patterns.

Table 1. All produced films' structural parameters were measured at a thickness of 400nm.

Samples	2 Theta (deg)	β (deg)	D_g (nm)	η x10^{-4} ($lines^2 \times m^{-4}$)	δ ($lines/m^2$)
Ag_2Te Pure	41.498	0.3464	25.62466	1.412311	1.52E+15
Ag_2Te: 1%Al	41.6184	0.2649	33.52193	1.079592	8.9E+14
Ag_2Te: 1.5%Al	41.6097	0.2391	37.13802	0.974473	7.25E+14

Figure 2**.** The impact of doping on Ag_2Te and Ag_2Te:Al film was demonstrated by calculating the surface topographic of pure Ag_2Te- doping with 1% and 1.5%. The XRD test findings and the particle size agree. Table 2 displays all of the produced films' particle sizes, surface roughness, and root mean square roughness values[15].

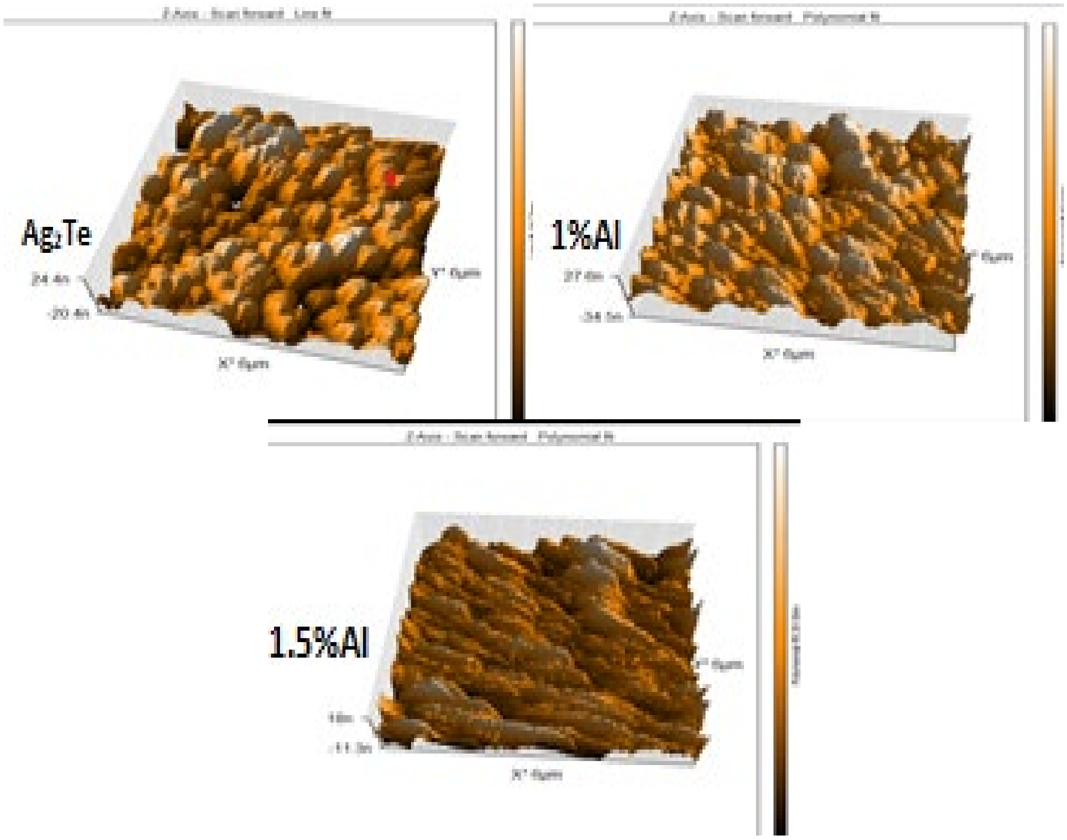

Fig. 2. (3D) AFM images of all films were prepared.

Table 2. All films' AFM information was created.

Sample	Size of grain (nm)	Roughness. (nm)	Root mean square. (nm)
Ag_2Te	38.49	7.49	10.01
Ag_2Te:1%Al	41.75	15.87	20.14
Ag_2Te:1.5%Al	43.68	16.63	22.14

Figure 3:The surface morphology of all samples of pure (Ag_2Te) films and doped with (Al) was examined using (FESEM) technique with a magnification of 120 KX in order to know the nature of the film surfaces and to clarify the change in the particle size, as the pictures in Figure (3) show that impurities have additives in certain proportions have a great effect on the formation of the surface composition of the prepared films, and all the prepared films have granules with a uniform distribution, and when the percentage of doping is increased, the surface of the film is more homogeneous and regular, and thus the quality of the prepared films improves, and also the increase in the percentage of doping led to a change in the particle size as a result of the effect of impurity atoms included in the composition of the material, which indicates that increasing the percentage of doping with (Al) leads to a change in the shape of the particles crated as a result of superposition[16].

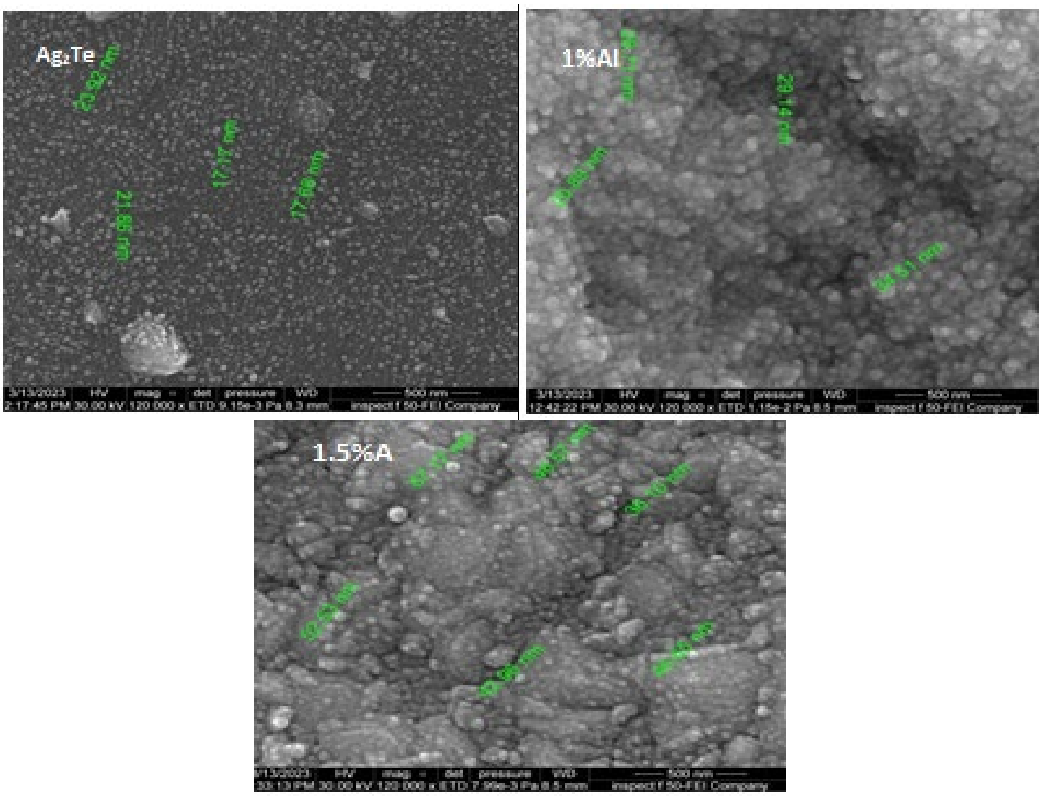

Fig. 3. FESEM images s of all films were prepared.

3.2. Optical properties

Figure 4 for the studied Ag_2Te and Al-doped Ag_2Te thin films with a thickness of 400 nm, It demonstrates how wavelength (λ) affects absorbance in the spectral area between 400 and 1000 nm. In the figure, the films exhibit greater absorbance on the side of shorter wavelength (UV) and less absorbance on the side of longer wavelength (visibility) and we note that the absorbance edges move to large wavelengths (red_shift). Showing the photonic gap decreases with rising Al concentration. This is because there are runaway transitions in the density state in the energy gap, The sharp absorption edge opposite the band gap confirms the good quality of the as-grown films, The incoming photons in the low_wavelength region have enough energy to excite electrons from the valance bands to the conducting bands and these photons are eventually absorbed by the material[17]. The photon will move because it lacks sufficient energy to interact with the atom at high wavelength. The thickness of 300nm films is measured.

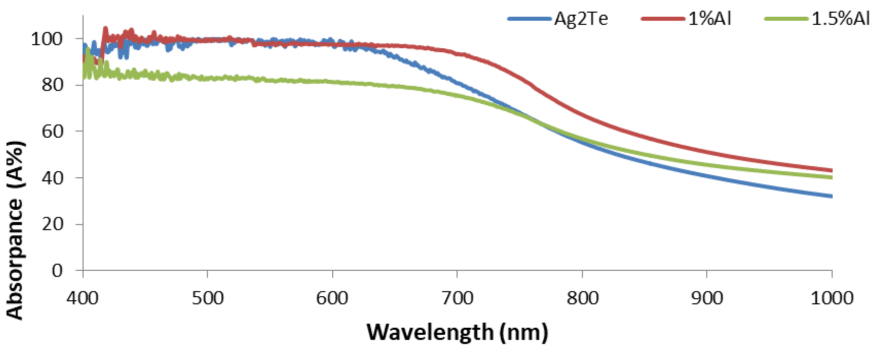

Fig. 4. Optical absorption Each film's VS wavelength was created.

Fig. 5 illustrates how optical absorption coefficient changes with wavelength for the investigated of pure Ag_2Te and Al doped Ag_2Te films at the spectral range from 400nm to 1000 nm. founded on the fact that an increase in the dopant led to a little change in absorption values, as the concentration of Al rises, the values of the optical absorption coefficient rise as well. All films in the high absorption region have values more than 10^4 cm^{-1}, which raises a direct transmission's probability.

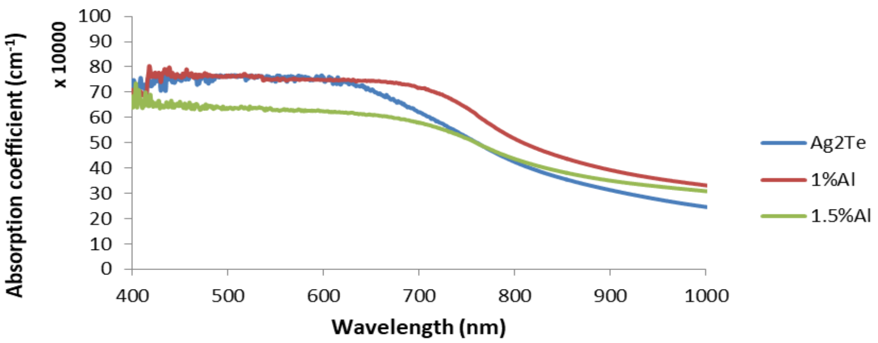

Fig. 5. The absorption coefficient of all films were prepared.

Fig. 6 Drawing the curves to $(\alpha h\nu)^2$ = 0 for Ag_2Te and 1% and 1.5% from Al doped Ag_2Te film yielded optical energy gap values of 1.4, 1.34, and 1.26 eV, respectively**.** It is possible to determine the optical energy gap of the intercept $(\alpha h\nu)^2$ VS. Photon energy hν for allowed direct transition . The experimental values of αhν against Ag_2Te and Ag_2Te containing 1% and 1.5% of Al are presented It is noted from Figure (6) the added impurity atoms led to a decrease in the value of the optical energy gap for all prepared films. This is due to the density of donor levels formed by the added impurity atoms near the conduction band .Thus, the appearance of the decrease in the value of the energy gap, although it was not large in its amount, is attributed to some of the impurity atoms added has worked on the treatment of point defects (filling fungal voids) present in The crystal structure of the compound was better, so its work was limited to improving the crystal structure and filling Lattice voids more than contribute to changing the value of the energy gap by a large amount.

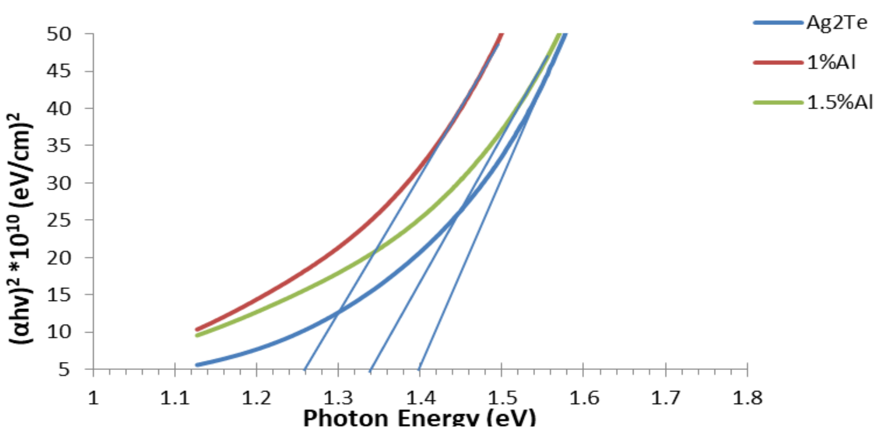

Fig. 6. A Plot of $(\alpha h\nu)^2$ VS. Photon energy (hν) for each film was created.

4. Conclusion

According to XRD results, thin films of Ag_2Te and Al doping that were 1% and 1.5% respectively, were polycrystalline and having a monoclinic structure. The film surface is extremely smooth, according to the AFM results. The roughness of the film surface rises with an increase in Al concentration. In the visible region, the absorption value of pure Ag_2Te and Al doping film reaches 90%, which is significant for its uses as solar cells, The optical energy gap of pure Ag_2Te thin films and containing 1% of Al and 1.5% of Ag_2Te was equal to 1.4, 1.34, 1.26 eV.

References

[1] Maki, S.A., A.A. Shehab, and A.A. Salih, Ibn AL-Haitham Journal For Pure and Applied Science, 2017. 27(3): p. 278-290.
[2] Ali, H.M. and I. Khudayer, Journal of Ovonic Research, 2022. 18(5); https://doi.org/10.15251/JOR.2022.185.675
[3] Gupta, S., et al., Journal of The Institution of Engineers (India): Series D, 2022: p. 1-10; https://doi.org/10.1007/s40033-022-00363-9
[4] Abbas, E.A., Ibn AL-Haitham Journal For Pure and Applied Science, 2020. 33(2): p. 11-18; https://doi.org/10.30526/33.2.2438
[5] Yuan, Z., et al., Sensors and Actuators B: Chemical, 2022. 363: p. 131790; https://doi.org/10.1016/j.snb.2022.131790
[6] Abdullah, M., et al., Energy & Fuels, 2023; https://doi.org/10.1021/acs.energyfuels.2c03279
[7] Kalantar-Zadeh, P., M. Mousavi, and D. Tang, Control of Composition and Morphology of Metal Telluride Compounds Synthesized Using a Liquid Metal-Based Technique. Jianbo, Control of Composition and Morphology of Metal Telluride Compounds Synthesized Using a Liquid Metal-Based Technique.
[8] Mustafa, M.H., Ibn AL-Haitham Journal For Pure and Applied Science, 2017. 27(3): p. 273-278.
[9] Xaba, T., et al., A Facile One-Pot Synthesis of Ag2te Nanoparticles and the Fabrication of Nanocomposites for the Removal of Chromium (Vi) in Wastewater. Available at SSRN 4391416.
[10] Ali, H.M. and I. Khudayer, Chalcogenide Letters, 2023. 20(3): p. 197-203; https://doi.org/10.15251/CL.2023.203.197
[11] Mazban, R.G. and I.H. Khudayer. AIP Conference Proceedings. 2020. AIP Publishing LLC; https://doi.org/10.1063/5.0033127
[12] Cao, L., et al., ACS Applied Materials & Interfaces, 2022. 14(42): p. 48296-48302; https://doi.org/10.1021/acsami.2c15270
[13] Gupta, S., et al., Journal of Materials Engineering and Performance, 2022. 31(10): p. 7945-7954; https://doi.org/10.1007/s11665-022-06864-8
[14] Sobhi, S. and B. Hussein, Chalcogenide Letters, 2022. 19(6): p. 409-416; https://doi.org/10.15251/CL.2022.196.409
[15] Ajar, S.H., et al., Ibn AL-Haitham Journal For Pure and Applied Science, 2017. 28(2): p. 41-51.
[16] Mahdi, M., Journal of College of Education, 2010(5).
[17] Hamdi, S.S., Eng. &Tech. Journal, 2016: p. 2443-2449; https://doi.org/10.30684/etj.34.13A.7